Skeletal Myoblast Transplantation for Repair of Myocardial Necrosis

Charles E. Murry,* Robert W. Wiseman,‡ Stephen M. Schwartz,* and Stephen D. Hauschka§
**Department of Pathology,* ‡*Department of Radiology, and* §*Department of Biochemistry, University of Washington School of Medicine, Seattle, Washington 98195*

Abstract

Myocardial infarcts heal by scarring because myocardium cannot regenerate. To determine if skeletal myoblasts could establish new contractile tissue, hearts of adult inbred rats were injured by freeze-thaw, and 3–4.5 $\times$ 10^6 neonatal skeletal muscle cells were transplanted immediately thereafter. At 1 d the graft cells were proliferating and did not express myosin heavy chain (MHC). By 3 d, multinucleated myotubes were present which expressed both embryonic and fast fiber MHCs. At 2 wk, electron microscopy demonstrated possible satellite stem cells. By 7 wk the grafts began expressing β-MHC, a hallmark of the slow fiber phenotype; coexpression of embryonic, fast, and β-MHC continued through 3 mo. Transplanting myoblasts 1 wk after injury yielded comparable results, except that grafts expressed β-MHC sooner (by 2 wk). Grafts never expressed cardiac-specific MHC-α. Wounds containing 2-wk-old myoblast grafts contracted when stimulated ex vivo, and high frequency stimulation induced tetanus. Furthermore, the grafts could perform a cardiac-like duty cycle, alternating tetanus and relaxation, for at least 6 min. Thus, skeletal myoblasts can establish new muscle tissue when grafted into injured hearts, and this muscle can contract when stimulated electrically. Because the grafts convert to fatigue-resistant, slow twitch fibers, this new muscle may be suited to a cardiac work load. (*J. Clin. Invest.* 1996. 98:2512–2523.) Key words: myocardial infarction • skeletal myoblast • myosin heavy chain • contractile function • cell transplantation

Introduction

Experimental and clinical therapies for myocardial infarction have focused traditionally on limiting infarct size. Unfortunately, the goal of limiting myocardial injury has been difficult to achieve clinically, because ischemic myocardium dies quite rapidly (1) and most patients wait more than 3 h after coronary occlusion before seeking medical attention. As an alternative approach, we are exploring strategies to induce the injured heart to heal with muscle replacement rather than forming scar tissue.

Address correspondence to Charles E. Murry, M.D., Ph.D., Department of Pathology, Box 357470, Room E-520, HSB, University of Washington School of Medicine, Seattle, WA 98195. Phone: 206-616-8685; FAX: 206-543-3644; E-mail: murry@u.washington.edu

Received for publication 18 April 1996 and accepted in revised form 2 October 1996.

J. Clin. Invest.

0021-9738/96/12/2512/12 $2.00
Volume 98, Number 11, December 1996, 2512–2523

One strategy for muscle regeneration is to transplant either skeletal or cardiac myocytes into the injured heart. Studies from Field's group showed that cardiac myocytes can be transplanted into normal hearts, where they couple with host cardiocytes via intercalated discs (2, 3). However, a major drawback to using cardiocytes is their inability to proliferate in culture. At present it seems unlikely that enough primary cardiocytes could be obtained from the patient or histocompatible donor to repair a myocardial infarct in humans. On the other hand, skeletal muscle satellite cells (muscle stem cells) proliferate well in culture. Satellite cells could be obtained from muscles of infarct patients and rapidly expanded in culture, or stocks of potentially therapeutic myoblasts could be obtained from embryos and frozen for subsequent use (4, 5). Furthermore, physiological studies have shown that when properly conditioned, skeletal muscle can adapt to perform a cardiac-type work load (6). Recent studies have demonstrated the feasibility of grafting skeletal myoblast lines into normal hearts (7) and autologous satellite cells into injured hearts (8, 9). However, to generate significant amounts of functional new muscle the transplanted cells ideally should proliferate and then differentiate into mature myofibers capable of sustaining a cardiac work load. This study was performed to determine the proliferation and differentiation patterns of skeletal myoblasts after engraftment into injured rat hearts and to determine whether this new muscle could support contractile activity.

Methods

Skeletal myoblast isolation and culture. These studies were approved by the University of Washington Animal Care Committee and were conducted in accordance with federal guidelines. Skeletal myoblasts were obtained from the limbs of 1–3-d-old Fischer rats. This inbred strain was used to avoid immune barriers to transplantation. After time of killing, the carcasses were skinned and the limbs were placed into cold tissue culture media. Under a dissecting microscope, the muscles were stripped of surrounding adipose tissue and fascia and bluntly dissected from their tendons. The muscles were minced with iridectomy scissors until a fine slurry was formed. The slurry was then digested in 0.05% trypsin/EDTA (GIBCO-BRL, Gaithersburg, MD) in Ham's saline A at 37°C, with intermittent mechanical agitation to assist dispersal. After 30–45 min the cell suspension was filtered through sterile gauze to remove undispersed tissue fragments and rod shaped mature myofibers. Cells were plated at $\sim 5 \times 10^6$ cells/dish in 100-mm gelatinized plates in 10 ml Ham's F10C media, containing 15% horse serum and 50 μg/ml gentamicin sulfate (Gemini Bioproducts, Inc., Calabasas, CA). Recombinant human basic fibroblast growth factor was added twice daily to a final concentration of 6 ng/ml, and the complete medium was replaced once per day. Approximately 10% of the cells attached and grew with a doubling time of $\sim$ 18 h. The cultures contained a mix of small, oval myoblasts and elongated, spindle-shaped cells consistent with fibroblasts. Subconfluent cultures were passaged every 2–3 d (1:5 split) to minimize the occurrence of myogenic differentiation at higher density. On the day before transplantation, the cultures were tagged for subsequent identification in vivo. In some experiments cells were tagged with fluorescent micro-

spheres (1:500 dilution of stock 200 nm yellow-green fluorescent microspheres; Molecular Probes, Eugene, OR). The latex microspheres were endocytosed (typically > 20 spheres/cell) and served as cytoplasmic markers (10). In other experiments, cells were incubated overnight with [^{3}H]thymidine (1 μCi/ml) to mark their nuclei after autoradiography. Cultures were trypsinized immediately before transplantation and suspended at a concentration of $\sim 3 \times 10^7$/ml. Small aliquots of the remaining cell suspension were replated at $\sim 2 \times 10^4$ cells/cm^2 into gelatinized, multichamber plastic slides, and fixed in methanol after various culture intervals for immunostaining.

Rat cardiac injury models. Inbred male Fischer rats (Simonsen Labs, Gilroy, CA) weighing 350–400 grams were anesthetized with intraperitoneal ketamine-xylazine (68 and 4.4 mg/kg, respectively), intubated, and mechanically ventilated with room air. The heart was exposed aseptically via a left thoracotomy, and a 1-cm-diameter aluminum rod, precooled with liquid nitrogen, was placed in direct contact with the anterior left ventricle for 15 s. Freeze-thaw reproducibly caused a disc-shaped region of coagulation necrosis, $\sim$ 1 cm in diameter, extending $\sim$ 2 mm into the myocardium. It should be noted that while infarcts typically have irregular borders with viable peninsulas of subepicardial myocardium along penetrating vessels, freeze-thaw lesions consist of confluent necrosis in the subepicardium with viable myocardium in the subendocardium. Because they are not transmural, freeze-thaw lesions do not cause cardiac aneurysm formation. Despite these differences, the cellular patterns of coagulation necrosis, inflammation and phagocytosis, granulation tissue formation, and scarring after freeze-thaw injury are indistinguishable from myocardial infarction (11–13), making it a suitable model to study myocardial repair.

In the initial studies, $\sim 3 \times 10^6$ myoblasts in 100 μl tissue culture media were injected superficially into the center of the injured region immediately after injury, using a 27-gauge needle. Then, the chest was closed and the rats were allowed to recover for timed intervals from 1 d to 3 mo (n = 4/time point). To mimic a clinical situation more closely, a second protocol was used in which the freeze-thaw lesion was allowed to heal for 1 wk before transplanting myoblasts. By 1 wk, most of the necrotic myocardium had been replaced by granulation tissue, but scar formation had not yet begun. The rats (n = 2/time point; no 3 d or 3 mo time points) were reanesthetized and a thoracotomy was repeated. The heart was exposed and a 100-μl suspension containing $\sim 3 \times 10^6$ myoblasts was injected into the wound as described above. The chest was closed and the animals were allowed to recover for intervals from 1 d to 7 wk.

To detect DNA synthesis in the grafts the rats were treated with the thymidine analogue 5-bromo-2′-deoxyuridine (BrdU)[1] (Boehringer-Mannheim, Indianapolis, IN). 1 d before time of killing, the rats were lightly anesthetized, and a 50-mg tablet of BrdU was implanted subcutaneously for measurement of cell replication. Preliminary studies showed that a subcutaneous 50-mg BrdU tablet gave comparable replication rates to a 24-h continuous infusion with an osmotic mini-pump (not shown). For rats killed 1 d after transplantation, a single 10-mg pulse of BrdU was given intraperitoneally 1 h before time of killing. This avoided incorporation of BrdU into the cells which were cycling at the time of transplantation.

Rats were killed with a pentobarbital overdose and their hearts were excised. In the immediate transplantation groups, the aorta was cannulated and the hearts were perfusion fixed with methyl Carnoy's solution (60% methanol, 30% chloroform, 10% glacial acetic acid), transversely sectioned, and embedded in paraffin by routine methods. In groups transplanted 1 wk after injury, the hearts were transversely sectioned, embedded in OCT (Miles Inc., Kankakee, IL), and frozen in a dry ice–ethanol bath for frozen section analysis. In both protocols, sections of gut were obtained as controls for measurement of cell replication with BrdU.

Measurement of contractile function in isolated wound strips. Rat hearts were given 4.5×10^6 myoblasts (n = 8) in 100 μl or a sham injection of saline (n = 3) immediately after injury. 2 wk after engrafting, the hearts were excised and transversely sectioned. Under a dissecting microscope, most of the subendocardial myocardium was trimmed away from the injured region, and isolated wound strips ($\sim 1.5 \times 1.5 \times 8$ mm) were prepared. One or two strips were studied from each myoblast-engrafted heart, and two or three strips were studied from each sham-injected heart. The strips were ligated at both ends with silk suture and then placed in a bath of physiological saline with the following composition (mmol/liter): 116 NaCl, 4.6 KCl, 1.2 $MgSO_4$, 2.5 $CaCl_2$, 26 Mops (pH 7.4), 11 glucose, and 10 mg/liter gentamicin. The buffer was equilibrated with 95% O_2/5% CO_2 and maintained at 20°C via a thermostatically controlled water jacket. Wound strips were mounted between an isometric force transducer (model 60-2995; Harvard Apparatus, Inc., South Natick, MA) and a fixed glass hook. Resting tension was set initially at 0.5 g. Strips were stimulated with 1-ms bipolar pulses delivered via platinum wire electrodes using a Grass model S48 stimulator (Astro-Med, Inc., West Warwick, RI). Voltage was increased in 10-V increments until contractile activity was observed. Force traces were displayed on a digital storage oscilloscope (model 3091; Nicolet Instrument Corp., Madison, WI) and recorded using a General Scanning model RS4-5P strip chart recorder. After determining the force–voltage relationship, the optimal length for force production was determined for each wound strip using test contractions at 2-min intervals, a time sufficient for metabolic recovery in mammalian fast twitch muscles (14). Force–frequency analysis was performed by increasing the stimulation frequency in 1-Hz increments; tetanus was defined as the point where the oscillations of contractile force at the plateau were < 3% of the net force generated (14). Finally, to test fatigability the grafts were subjected to a simulated cardiac-like duty cycle, consisting of 0.33 s of tetanus followed by 0.67 s of relaxation (1:2 cycle), continuing for 6 min. After completion of functional studies the strip's cross-sectional area was determined, and the tissue then was processed for histology or electron microscopy.

Immunocytochemistry. Antibodies used for immunostaining are given in Table I. 6-μm frozen sections were cut on a cryostat, briefly air dried, and stored at −70°C until use. 5-μm paraffin sections were deparaffinized in xylene and rehydrated in a graded alcohol series. Cultured cells were fixed and stored in cold PBS until use. For all samples, endogenous peroxidase activity was quenched by incubating with 0.3% H_2O_2 in methanol for 30 min. Immunostaining was carried out at room temperature. Sections were blocked with 1.5% normal horse serum in PBS for 1 h. The sections were then incubated with the primary antibody in 1.5% horse serum for 1 h, followed by incubation with the secondary antibody (rat adsorbed horse anti–mouse, 1:400 dilution; Vector Labs, Inc., Burlingame, CA) for 1 h. Antigens were localized with an avidin-biotin-peroxidase complex (ABC Elite kit; Vector Labs). For staining with a single antibody, diaminobenzidine (Sigma Immunochemicals, St. Louis, MO) was used as a chromagenic substrate. For double immunolabeling with antibodies to myosin and BrdU, sections were first exposed to 1.5 N HCl for 15 min at 37°C to denature the DNA, followed by a rinse in 0.1 mol/liter borax to stabilize the denatured strands. Sections were then stained routinely for myosin heavy chain (MHC) using diaminobenzidine. After a second quenching in 0.3% H_2O_2, sections were blocked with 1.5% normal horse serum, and then incubated with a mouse monoclonal antibody to BrdU for 1 h. After incubation with the secondary antibody (horse anti–mouse), BrdU was localized with an avidin-biotin-peroxidase complex, using True Blue (KPL, Gaithersburg, MD) as substrate. Cross-reactivity between the first primary antibody and the second secondary antibody did not occur, as long as the True Blue substrate was incubated for a short duration (< 1 min). Sections were counterstained either with methyl green, nuclear fast red, or hematoxylin.

Electron microscopy. After measurement of contractile function, one of the tissue strips was immersed in half strength Karnovsky's fix-

1. *Abbreviations used in this paper:* BrdU, 5-bromo-2′deoxyuridine; MHC, myosin heavy chain.

Table I. Antibodies Used for Immunocytochemistry

Antibody	Antigen recognized	Dilution	Source	Reference
MF-20	Sarcomeric MHCs	Hyb. Sup., 1:100	American Type Culture Collection, Rockville, MD	39
MY-32	Skeletal MHC-fast (types IIA and IIB)	Mouse ascites, 1:2000	Sigma Immunochemicals	40
BA-G5	Cardiac MHC-α	Hyb. Sup., 1:5	American Type Culture Collection	41
F1.652	Embryonic MHC	Hyb. Sup., 1:100	Developmental Studies Hybridoma Bank*	42
A4.951	β-MHC	Hyb. Sup., 1:50	American Type Culture Collection	43
Anti-BrdU	BrdU	IgG, 1:50000	Eurodiagnostics, Apeldoorn, The Netherlands	44

IgG, purified IgG monoclonal antibody; *Hyb. Sup.*, hybridoma supernatant. * The monoclonal antibody F1.652, developed in the laboratory of Dr. Helen Blau, was obtained from the Developmental Studies Hybridoma Bank maintained by the Department of Pharmacology and Molecular Sciences, Johns Hopkins University School of Medicine, Baltimore, MD, and the Department of Biological Sciences, University of Iowa, Iowa City, IA, under contract NO1-HD-2-3144 from the National Institute of Child Health and Human Development.

ative and dissected into small cubes < 1 mm in greatest dimension. The tissue was fixed overnight in half strength Karnovsky's fixative, postfixed for 1 h in 1% osmium tetroxide at room temperature, dehydrated through a graded alcohol series followed by propylene oxide, and embedded in Medcast resin (Ted Pella, Inc., Redding, CA). Semithin sections were stained with toluidine blue and examined by light microscopy. Thin sections were cut from selected blocks, stained with lead citrate and uranyl acetate, and examined in a Jeol JEM 1200EXII transmission electron microscope. Representative areas were photographed.

Results

Characteristics of myoblast cultures. The muscle cultures contained a mixed cell population. At least 22% of the cells were skeletal muscle, as indicated by their staining for sarcomeric myosin after switching to a differentiation medium containing 1.5% serum and no FGF for 3 d. This procedure underestimates the true percentage of skeletal muscle cells by severalfold, since the nonmyogenic cells continue to divide after the medium switch while the myoblasts complete their present cell cycle and then terminally differentiate. Approximately 1% of the cells stained with antibodies to smooth muscle α-actin, which can mark either smooth muscle cells or fibroblasts. Virtually none of the cells stained with an antibody for the endothelial marker von Willebrand factor. The remaining cells were presumably fibroblasts.

Histology and differentiation patterns of myoblast grafts. Cultured skeletal myoblasts were transplanted into cardiac freeze-thaw lesions either immediately after injury, or, to mimic a clinical situation more closely, cells were transplanted 1 wk after injury. The two protocols yielded similar results and will be described together; minor differences are noted below. On the first day after transplantation the myoblasts were mononuclear cells (Fig. 1 *A*). The grafted cells could be distinguished clearly from inflammatory cells within the necrotic tissue by their larger size and characteristic oval shape. (Fibroblast ingrowth from the surrounding tissue had not yet begun at this time.) The identity of the grafted cells was confirmed by their cytoplasmic fluorescent microspheres and radioactive nuclei (not shown). Mitotic figures were common. The grafted cells did not stain with antibodies to skeletal or cardiac MHCs (Fig. 1 *B*). Thus, muscle differentiation had not yet occurred.

By 3 d after transplantation, many of the grafted cells had fused to form multinucleated myotubes (Fig. 1 *C*). Myotubes were partially aligned along the short (transverse) axis of the heart. The myotubes stained with antibodies to sarcomeric MHC, embryonic MHC (Fig. 1 *D*), and to MHC-fast (not shown). Occasional cross-striations were noted, but these were not frequent at this time (Fig. 1 *D*). The myotubes did not express cardiac MHC-α. By 1 wk the grafts were easily recognizable as skeletal myofibers and many cells contained cross-striations. As before, the new myofibers stained with antibodies to sarcomeric MHC, embryonic MHC, and MHC-fast, but did not express cardiac MHC-α (not shown). By 2 wk after transplantation the grafts had the appearance of maturing skeletal myofibers (Fig. 1 *E*). Sarcomeres were well formed, and many cells had peripheral nuclei. The myofibers stained intensely with antibodies to sarcomeric myosin, embryonic MHC (Fig. 1 *F*), and skeletal MHC-fast (Fig. 1 *G*). No staining with cardiac MHC-α antibodies was observed at 2 wk.

At 7 wk after transplantation the grafts were islands of mature skeletal muscle within young scar tissue (Fig. 1, *H–J*). There was a moderate increase in cell diameter compared with 2 wk. None of the muscle grafts were infiltrated or splayed apart by scar tissue, nor was there evidence of fiber atrophy. Vascular density appeared normal for muscle tissue (Fig. 1 *J*). All of the 7-wk grafts stained strongly with antibodies to sarcomeric myosin and embryonic MHC (Fig. 1 *H*). The grafts injected immediately after injury stained intensely with antiskeletal MHC-fast, comparable with Fig. 1 *F*. In contrast, the grafts injected 1 wk after injury stained poorly with antiskeletal MHC-fast (see below). No staining with antibodies to cardiac MHC-α was observed in the grafts, while the adjacent myocardium stained intensely (Fig. 1 *I*).

At 3 mo after transplantation the grafts again had the appearance of mature skeletal muscle (Fig. 1 *K*). Most myofibers had peripheral nuclei, and vascular density appeared normal. Fiber diameter was generally larger than in the 7-wk group, indicating that the cells had hypertrophied between 7 wk and 3 mo (compare Fig. 1, *J* and *K*). In one heart, however, part of the graft was infiltrated by scar tissue which encircled individual myofibers and was associated with fiber atrophy (Fig. 1 *L*). The grafts continued to express embryonic MHC and MHC-fast (not shown). Once again, no staining with antibodies to cardiac MHC-α was observed (comparable with Fig. 1 *I*). At all time points the myofibers were predominantly aligned parallel with the short (transverse) axis of the heart and therefore appeared in longitudinal section. However, some fascicles of muscle appeared obliquely or cross-sectioned in this plane.

In summary, the grafts began to differentiate into myo-

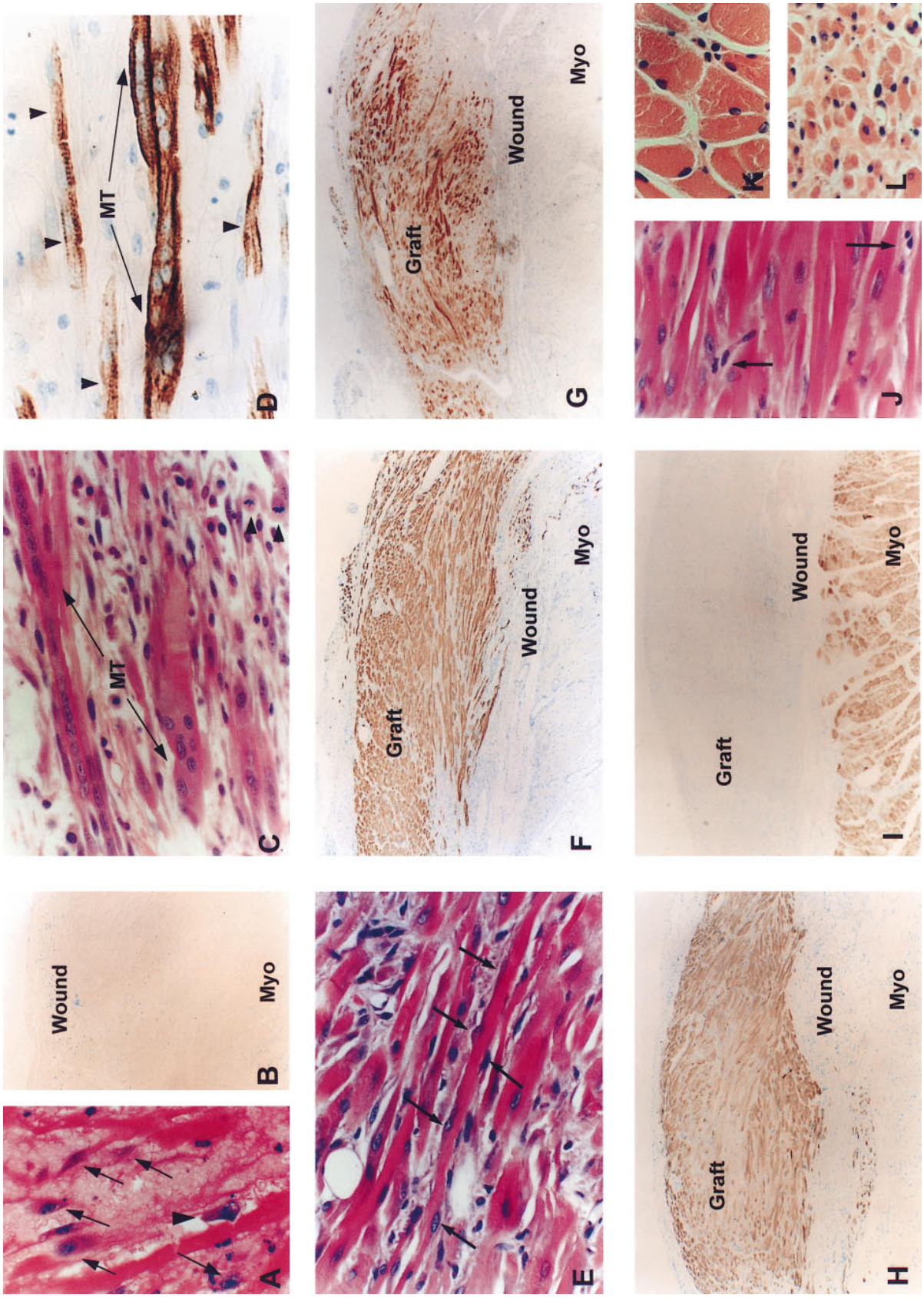

Figure 1. Morphology and MHC expression in skeletal myoblast grafts. Rat hearts were injured by freeze-thaw and syngeneic skeletal muscle cells were grafted into the lesions. All panels in this figure are from hearts which were grafted immediately after injury. (*A*) 1-d graft. The grafted cells are identifiable as relatively large, oval shaped cells (*arrows*) within the necrotic myocardium. One graft cell is in mitosis (*arrowhead*). Numerous smaller inflammatory cells are present within the lesion. Fibroblast ingrowth from surrounding viable tissue had not yet begun at this

tubes between 1 and 3 d and acquired the appearance of maturing myofibers with well formed sarcomeres by 2 wk. The grafts expressed both embryonic MHC and MHC-fast at all times between 3 d and 3 mo. There was no expression of cardiac MHC-α at any time.

Electron microscopy. Electron microscopy was performed on one heart, 2 wk after myoblast grafting. Most of the grafted cells had well formed, slightly contracted sarcomeres which were aligned in registry (Fig. 2 *A*). Mitochondria were abundant. Multinucleation was evident in many cells, as were well formed T-tubules. However, in other cells a spectrum of morphological stages was present, consistent with developing skeletal muscle (Fig. 2 *B*). Cells at the earliest stage were small, had scanty myofibril content, and contained focal aggregations of electron-dense material suggestive of developing Z-discs. In these cells there were abundant ribosomes and glycogen, a prominent Golgi apparatus, and dilated segments of sarcoplasmic reticulum. Intermediate cells were larger and had increasing amounts of myofibrils with a corresponding decrease in ribosomes and glycogen. Some cells had well formed sarcomeres, but these were out of registry compared with the most mature cells. No intercalated discs were identified between cells in the graft region. Adjacent myofibers often had intimately apposed, interdigitating cell membranes. Occasional cells were identified with electron-dense membrane structures suggestive of intermediate adherens junctions and gap junctions (Fig. 2, *C* and *D*). Some mature myofibers were closely associated with mesenchymal cells, located within the basal lamina compartment of the myofiber. Their location within the basal lamina of the myofiber suggests that they might be new satellite stem cells (Fig. 2, *E* and *F*). Some of these mesenchymal cells had abundant rough endoplasmic reticulum, similar to fibroblasts. Cells with this morphology have also been described in regenerating skeletal muscle by Trupin et al. (15). Their location within the basal lamina of the myofiber and the absence of collagen in this space make it unlikely that these cells are actually fibroblasts.

Myoblast grafts convert from fast to slow twitch fibers. The poor staining for MHC-fast in the 7-wk group with delayed transplantation seemed at variance with the morphology of the grafts, which showed relatively hypertrophic cells with well formed sarcomeres. We hypothesized that the grafts had undergone fiber type conversion to slow twitch muscles, which no longer expressed high levels of MHC-fast. Slow twitch fibers have physiological similarities to cardiac muscle, including a high capacity for oxidative phosphorylation and fatigue resistance. Furthermore, slow fibers use β-MHC as a major contractile protein, which is also the predominant myosin in developing rat hearts. In contrast, fast twitch fibers use glycolysis for ATP production, have a low aerobic capacity and fatigue rapidly, and do not express β-MHC (16). Therefore, we compared β-MHC expression with skeletal MHC-fast, to determine fiber types in the maturing grafts.

At 1 wk the grafts stained intensely for MHC-fast (Fig. 3 *A*) but did not stain with an antibody to β-MHC (Fig. 3 *B*). At 2 wk the grafts continued to express MHC-fast. In the group transplanted immediately after injury no expression of β-MHC was noted at 2 wk, yet in grafts transplanted 1 wk after injury some cells expressed β-MHC (not shown). At 7 wk after transplantation the two groups differed in expression of MHC-fast, with strong staining in the immediate transplant group (see Fig. 1 *G*) and weak staining in the group where transplantation was delayed for 1 wk after injury (Fig. 3 *C*). However, both the immediate and delayed transplantation groups exhibited extensive staining for β-MHC at 7 wk after transplantation (Fig. 3 *D*). At 3 mo there was continued expression of β-MHC and MHC-fast in the immediate transplantation group; we did not study the delayed transplantation protocol at 3 mo. Thus, myoblast grafts appeared to be undergoing conversion from fast twitch to slow twitch fibers. Conversion appeared to take place

---

time. Hematoxylin and eosin stain. ×800. (*B*) Low magnification of 1-d graft stained for embryonic MHC. The freeze-thaw lesion (*Wound*) occupies approximately the upper 75% of the field, while residual subendocardial myocardium (*Myo*) is present in the lower 25%. None of the grafted cells express embryonic MHC, indicating no differentiation had taken place yet. Methyl green counterstain. ×80. (*C*) 3-d graft. Multiple multinucleated myotubes (*MT*) are present. Note that myotubes are already aligned in parallel. The surrounding tissue contains numerous fibroblasts (some of which may be of graft origin), macrophages, and capillaries, characteristic of granulation tissue. Two mitotic figures are present at the lower right (*arrowheads*). Hematoxylin and eosin stain. ×800. (*D*) 3-d graft stained for embryonic MHC. The multinucleated myotubes (*MT*) express embryonic MHC, indicated by brown staining. Note faint cross-striations present at the periphery of some myotubes (*arrowheads*). Comparable staining was seen using antibodies to MHC-fast (not shown). Methyl green counterstain. ×800. (*E*) 2-wk graft. Multinucleated myofibers are present and many have peripherally placed nuclei (*arrows*); most of these nuclei appear to be within the sarcolemma, although some may be immediately external. Cross-striations were readily seen under the microscope but appear faint in the photograph. Hematoxylin and eosin staining. ×800. (*F*) 2-wk graft stained for embryonic MHC. The myofibers of the graft stain vigorously for embryonic MHC, while the underlying granulation tissue (*Wound*) and subendocardial myocardium (*Myo*) do not stain. Methyl green counterstain. ×80. (*G*) 2-wk graft stained for fast fiber isoforms of MHC. There is intense staining of the engrafted myofibers (*Graft*), indicating that they exhibit a fast twitch phenotype. Note that the residual myocardium (*Myo*) beneath the graft does not stain, nor does the granulation tissue of the injured region (*Wound*). ×80. (*H*) 7-wk graft stained for embryonic MHC. The graft continues to stain vigorously for embryonic MHC. There is no staining in the underlying young scar tissue (*Wound*) or the residual subendocardial myocardium (*Myo*). Methyl green counterstain. ×80. (*I*) 7-wk graft stained for cardiac MHC-α. The skeletal myofibers of the graft do not express MHC-α, nor does the underlying scar tissue (*Wound*). This indicates that the grafted skeletal muscle does not show cardiac differentiation. The subendocardial myocardium (*Myo*) stains vigorously for MHC-α. Methyl green counterstain. ×80. (*J*) 7-wk graft. Mature myofibers are present. Most myofibers have peripheral nuclei. Cross-striations were readily apparent under the microscope, but again are faint in the photograph. Multiple capillaries are present within the muscle tissue (*arrows*). Hematoxylin and eosin stain. ×800. (*K*) 3-mo graft. The myofibers (obliquely and cross-sectioned) have peripheral nuclei and are closely apposed with little intervening extracellular matrix. The myofibers are hypertrophic compared with the 7-wk grafts (compare fiber diameter with *J*). Most 3-mo grafts had this appearance. Hematoxylin and eosin stain. ×800. (*L*) 3-mo graft. The myofibers (cross-sectioned) in this region are encased by dense scar tissue and are atrophic. Note the markedly diminished cell diameters compared with *K*. Such entrapment of myofibers by scar was seen in one region of one heart. Hematoxylin and eosin stain. ×800.

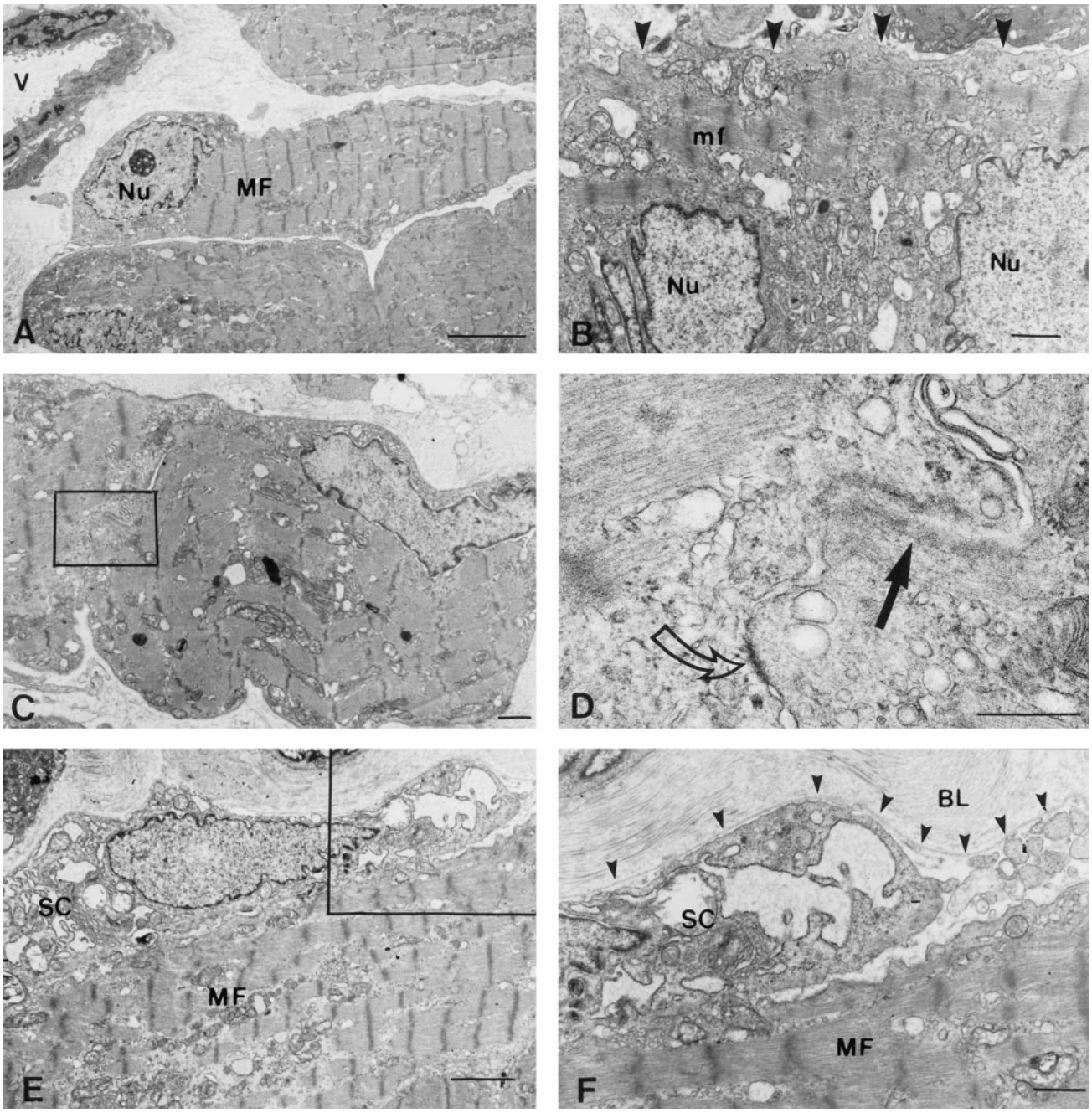

Figure 2. Transmission electron micrographs of 2-wk-old myoblast graft. The graft was placed immediately after cardiac freeze-thaw injury. (*A*) Low magnification overview showing well differentiated, striated skeletal myofibers (*MF*) within a collagen-rich matrix. A small venule (*V*) is shown at the left aspect. *Nu*, nucleus. Bar, 5 μm. (*B*) Moderately differentiated skeletal myofiber containing two nuclei (*Nu*), a modest complement of myofibrils (*mf*), and abundant ribosomes and sarcoplasmic reticulum between the nuclei. The sarcolemma is delimited by arrowheads. Bar, 1 μm. (*C*) Intercellular junction formation between adjacent myofibers. The two cells have closely apposed and interdigitated membranes. Two electron-dense plaques between the cells are present within the boxed region, suggestive of an adherens type intermediate junction and a gap junction, shown at higher magnification in *D*. Bar, 1 μm. (*D*) Higher magnification of the junctional region boxed in *C*, showing putative intermediate junction between adjacent myofibers (*solid arrow*) and gap junction (*open arrow*). Bar, 0.5 μm. (*E*) Skeletal myofiber (*MF*) with closely apposed mesenchymal cell atop it, suggestive of a satellite cell (*SC*). The boxed region is shown at higher magnification in *F*. Bar, 2 μm. (*F*) Higher magnification of region boxed in *E*. The putative satellite cell (*SC*) and the myofiber (*MF*) are contained within the same basal lamina compartment (*BL*, outlined by *arrowheads*). Although the cell has abundant rough endoplasmic reticulum, its location within the basal lamina of the myofiber and the absence of fibrillar collagen from this space make it unlikely that this is a fibroblast. Bar, 1 μm.

more rapidly when cells were transplanted into an injury with more advanced healing.

Proliferation of myoblast grafts. To identify cells undergoing DNA synthesis, the thymidine analogue BrdU was administered for 24 h before time of killing in most groups; animals in the day 1 group received a single pulse of BrdU 1 h before time of killing. Double immunostaining was performed with antibodies to the fast isoform of MHC and to BrdU, to detect

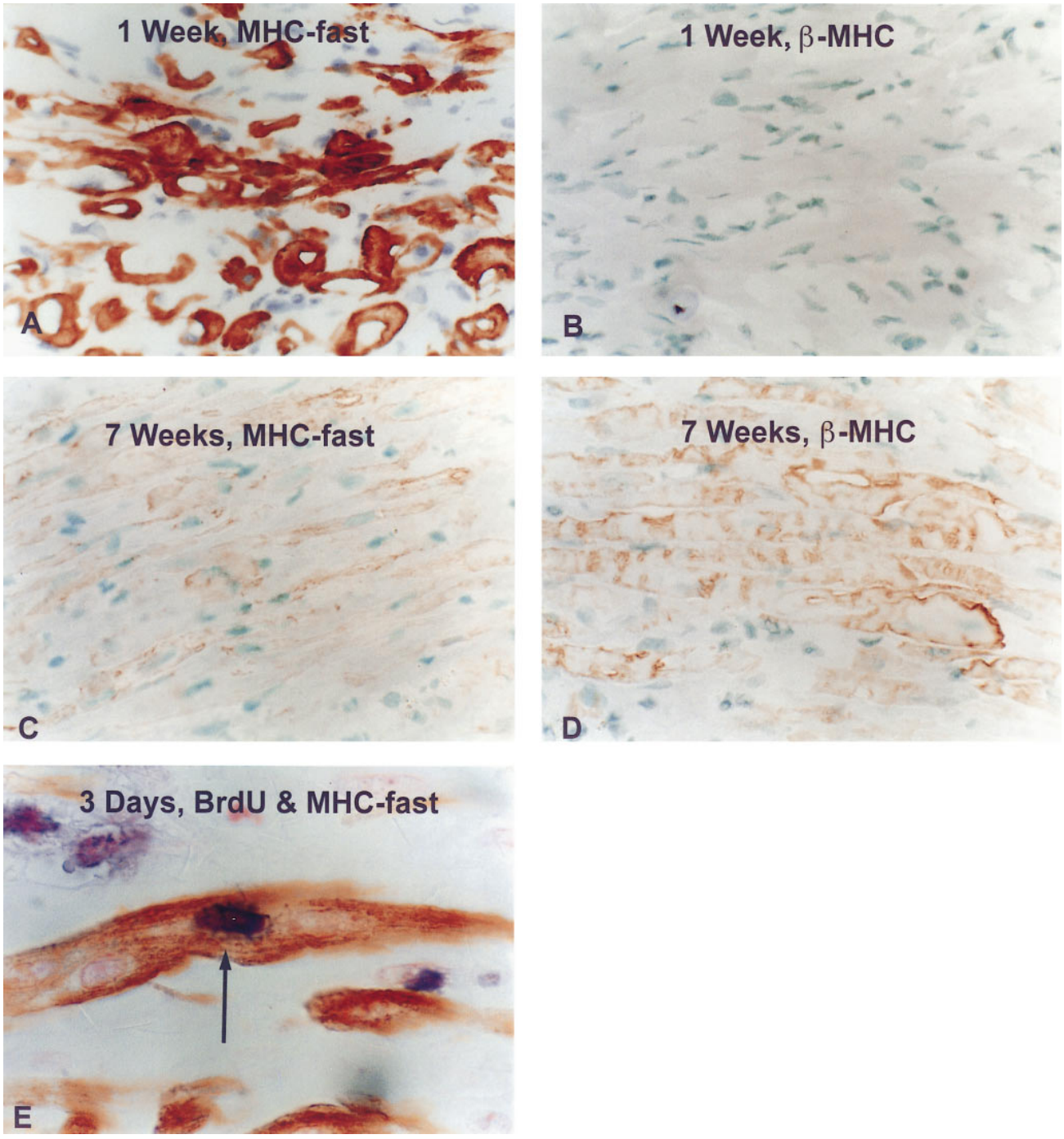

Figure 3. Fiber type conversion and proliferation of engrafted skeletal myoblasts. For the fiber typing experiments, rat hearts were injured by freeze-thaw and the lesions were allowed to heal for 1 wk. Syngeneic skeletal myoblasts were engrafted into the 1-wk-old wounds. For studies of cell proliferation, myoblasts were engrafted immediately after cardiac injury. Rats were killed at the indicated times after transplantation. Antibodies specific to fast twitch (MHC-fast) and slow twitch (β-MHC) fibers were used to define fiber types. Processing for frozen sections in *A–D* resulted in formation of contraction bands, artifactual clumping of the sarcomeres due to hypercontracture. BrdU was administered 24 h before time of killing to detect DNA synthesis. Double immunostaining for BrdU and MHC was then performed on paraffin sections. Appearance of a BrdU-positive nucleus within a myosin-positive cell indicated the myoblast had replicated and fused into the myotube within the last 24 h. (*A*) 1-wk graft stained for fast fiber isoforms of MHC. There is intense staining of the engrafted cells, indicating a fast fiber phenotype. Hematoxylin counterstain. ×960. (*B*) 1-wk graft stained with an antibody to the slow fiber-specific β-MHC. None of the grafted cells express β-MHC at this time, indicating that the cells show no characteristics of slow fibers. Methyl green counterstain. ×960. (*C*) 7-wk graft stained with an antibody to MHC-fast. There is weak staining compared with the 1-wk graft (*A*). Methyl green counterstain. ×960. (*D*) 7-wk graft stained with an antibody to β-MHC. The grafted cells now express β-MHC, indicating that they are acquiring a slow fiber phenotype (compare with *B*). Methyl green counterstain. ×960. (*E*) 3-d graft doubly stained for BrdU (purple) and MHC-fast (brown). One nucleus within the myotube stains purple (*arrow*), indicating it has undergone DNA replication before fusion into the myotube. The remaining nuclei in the myotube do not contain BrdU and pick up the red counterstain. Numerous myosin-negative cells in the surrounding wound tissue also stain positively for BrdU. Nuclear fast red counterstain. ×2,400.

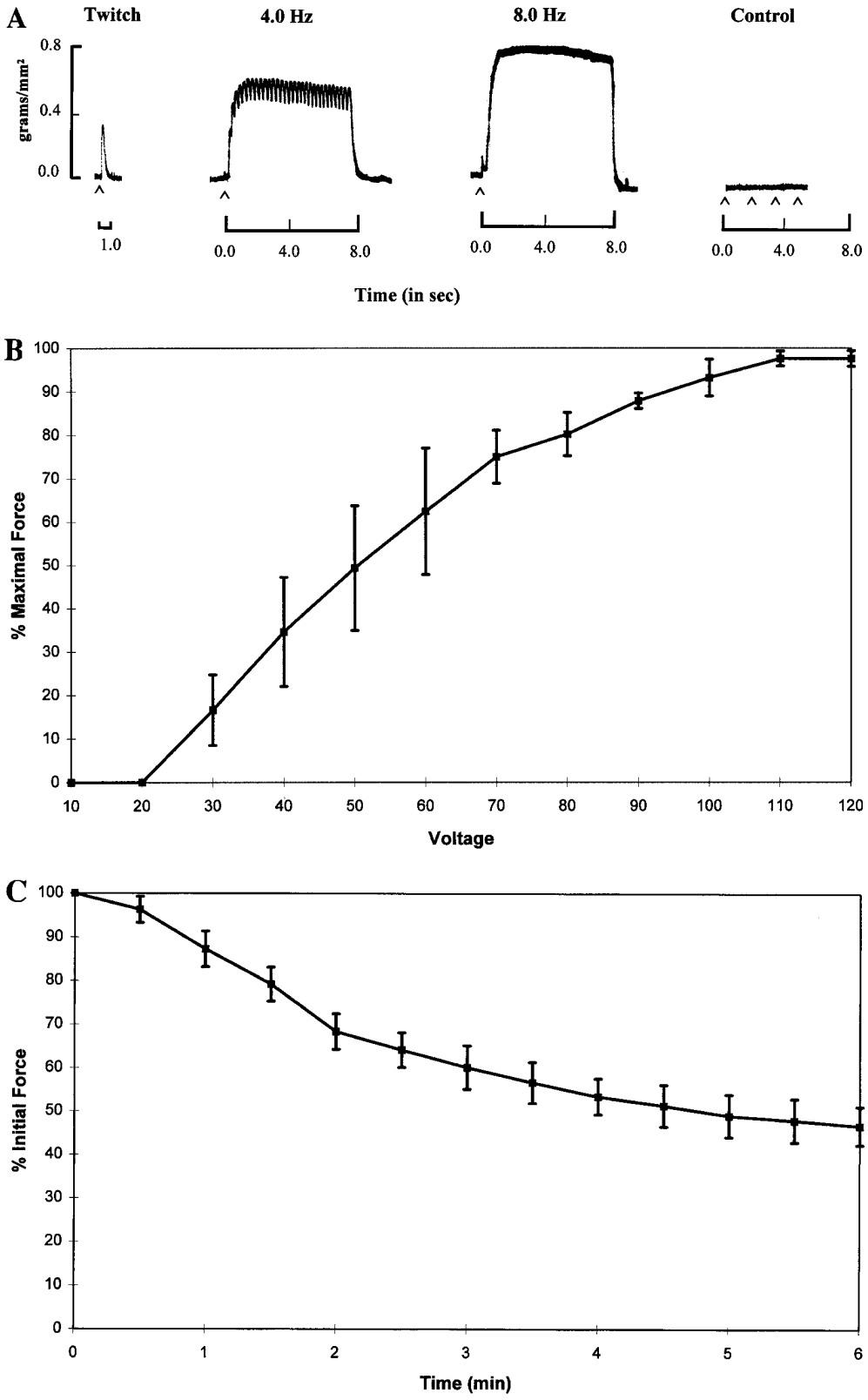

Figure 4. Contractile function of myoblast grafts ex vivo. Wound strips from injured hearts receiving either skeletal myoblasts or a sham saline injection were excised at 2 wk. Wounds were mounted on an isometric tension myograph in oxygenated buffer and electrically stimulated. The carats indicate the onset of electrical stimulation. Force has been normalized to cross-sectional area. (*A*) The first panel shows individual muscle twitch in a myoblast-injected wound. Note the rapid contraction and relaxation rates. The second panel shows that individual twitches began to superimpose with a stimulation frequency of 4 Hz, with a resulting potentiation in developed tension. The third panel shows that tetanus was induced with stimuli ≥ 7 Hz. Note the further increase in tension compared with the 4-Hz stimulation. Time to peak force in this preparation was ~ 1 s, faster than was typically observed for the overall group. The fourth panel shows that no tension was developed at any voltage in a sham-injected wound. This tracing is representative of six wound strips from three sham-injected hearts. (*B*) Force–voltage relationship. Developed tension for individual twitches increased as stimuli increased from 30 to 100 V, indicating recruitment of additional myofibers. Data have been normalized to maximal developed tension and are presented as mean±SEM of eight wound strips from six hearts. (*C*) Fatigue test. Wounds containing myoblast grafts were subjected to a cardiac-like duty cycle, consisting of repeated episodes of 0.33 s of tetanus/0.67 s of rest, to mimic a heart rate of 60 beats/min. There was a 53% decrease in developed tension at the end of the 6-min test. Note that most of the diminution in force occurred during the first 3 min. Data represent mean±SEM of seven wound strips from five hearts.

myoblasts which had proliferated and subsequently differentiated. In the day 1 grafts, proliferating cells were present within the necrotic lesion, which could have represented either graft cells or macrophages. As mentioned above, none of the cells expressed MHC at this time, so it was not possible to determine which among these were myoblasts (versus transplanted fibroblasts or host macrophages). In the day 3 grafts, occasional BrdU-positive nuclei were identified within myosin-pos-

itive cells (Fig. 3 *E*). We observed a total of 12 such nuclei in three hearts. No attempt was made to quantify this low rate, but it was certainly < 1% of total nuclei in myosin-positive cells. Virtually no BrdU-positive nuclei were seen in myosin-positive cells at 1, 2, or 7 wk after transplantation (not shown). We conclude that myoblast proliferation occurs for at least 3 d after grafting, but by 1 wk virtually all cells have ceased replicating.

Contractile function of myoblast grafts. The contractile properties of 2-wk-old myoblast grafts were determined by attaching isolated wound strips to a tension myograph ex vivo. Virtually no spontaneous mechanical activity was detected, consistent with the paucity of cardiomyocytes histologically. Electrical stimulation caused muscle twitches in six of eight myoblast-engrafted hearts (Fig. 4 *A*, *first panel*); strips from the remaining two hearts may have been damaged during sample preparation, since skeletal muscle was present histologically. The grafts showed a stepwise increase in tension development as voltage was increased from 30 to ~ 100 V with a plateau thereafter (Fig. 4 *B*). This indicates that increasing voltage recruited additional myofibers to contract, implying that the graft myofibers are electrically insulated from one another. It should be noted that cardiac muscle does not increase contractile force with increasing voltage, since cardiocytes are coupled electrically via gap junctions.

Next, force–frequency relationships were determined. Using 120% of the voltage required for maximal tension development, the frequency of stimulation was increased incrementally from 0.5 to 10 Hz. Twitches began to superimpose at frequencies of 3–4 Hz, with a resulting increase in total developed tension (Fig. 4 *A*, *second panel*). Fully fused tetani were produced with 6–7 Hz stimulation (Fig. 4 *A*, *third panel*). Peak force during tetanus was 1.98±0.45 grams (mean SEM); after normalization to cross-sectional area the peak force was 0.72±0.14 grams/mm^2. The time to peak tetanic force averaged 2.3±0.3 s, although 90% of peak force was typically generated within 1.5 s. The time to half-relaxation after tetanus was 240±17 ms. It should be stressed that tetanus cannot be induced in cardiac muscle, due to the long refractory period of cardiocytes.

Finally, a fatigue test was performed to test the response of this muscle to a cardiac-like work load. The grafts were subjected to a duty cycle consisting of repeated 0.33 s of tetanic stimuli followed by 0.67 s of rest, mimicking a heart rate of 60 beats/min. The grafts showed a 32% decline in developed tension by 2 min and a 53% decline by the end of the 6-min test period (Fig. 4 *C*). No contractile activity could be elicited from six of seven wound strips from three injured hearts which received a sham injection of saline instead of myoblasts (Fig. 4 *A*, *fourth panel*). In one sham heart an adhesion had developed between the heart and chest wall, resulting in a small amount of intercostal muscle adhering to one of the two wound strips. In this preparation we detected a peak force of 0.04 grams/mm^2, < 2% of what was present in the myoblast-engrafted hearts.

Thus, the skeletal muscle grafts could be stimulated to contract ex vivo and could sustain a cardiac-like duty cycle over a 6-min test period. Furthermore, the grafts showed two physiological properties unique to skeletal muscle: recruitment of fibers with increasing voltage and the ability to sustain tetanic contraction. We do not know yet whether the grafts contract in vivo.

Discussion

The principal findings of this study are: (*a*) neonatal skeletal myoblasts can be grafted into an injured heart; (*b*) the engrafted myoblasts initially proliferate and then begin to form multinucleated myotubes by day 3; (*c*) the myotubes differentiate into mature myofibers, which initially have a phenotype similar to fast twitch muscle; (*d*) the myofibers develop characteristics of slow twitch muscle as the wound heals; (*e*) the new muscle may form satellite stem cells; and (*f*) the new muscle can be stimulated to contract ex vivo.

Strategies for muscle regeneration after myocardial injury. In principal, there are at least three strategies to induce muscle regeneration after myocardial infarction. First, the surrounding cardiac myocytes could be stimulated to migrate into the wound and proliferate to repair the defect. There is evidence that a limited amount of cell replication by adult cardiocytes occurs naturally after myocardial infarction in humans (17) and in rats (18, 19), but the response is clearly not adequate to repair the defect. The factors responsible for cell cycle arrest in cardiocytes are not well enough defined at present to begin exploring this as a therapy. (The interested reader is referred to references 20–23 for further information on this topic.)

A second strategy is to induce the cells of cardiac granulation tissue (the fibroblast-rich tissue of wound repair) to differentiate into muscle rather than forming a scar. There is not enough known about cardiac differentiation at present to attempt formation of new myocardium. However, much more is known about skeletal muscle determination. The discovery of myogenic determination genes (24, 25) has made it possible to induce a wide range of cultured cell types to differentiate into skeletal muscle. Recent studies from our group (26) and others (27) have shown that cells in cardiac granulation tissue can be induced to differentiate into skeletal muscle by transfection with the prototype myogenic determination gene, MyoD. In these early experiments, however, the frequency of muscle differentiation has been low after MyoD gene transfer. Until the frequency of myogenic conversion can be increased, it will be difficult to investigate the functional properties of the MyoD-induced skeletal muscle.

The third strategy for muscular repair of infarcts is to transplant either skeletal or cardiac myoblasts into the injured region. Studies by Koh et al. (3) and Soonpaa et al. (2) have demonstrated that fetal cardiocytes will form intercalated discs with host cardiocytes, including gap junctions and adherens junctions, when transplanted into normal hearts. No proliferation was detected in the grafted cardiocytes. Less information is available on grafting of cardiocytes into injured hearts. Our group (28) and others (29, 30) have preliminary data showing that neonatal rat or fetal human cardiocytes can be transplanted successfully into injured rat hearts. To our knowledge there is no information regarding proliferation of these grafts, nor are any functional data available. As discussed above, the principal limitation to this approach is the inability to induce cardiocytes to proliferate in culture. Until cardiocytes can replicate in vitro, or proliferation-competent cells can be induced reliably to differentiate into cardiocytes, cardiocyte grafting will not be feasible in humans.

In contrast to cardiocytes, proliferating skeletal muscle precursors are readily available, either as primary myoblasts in developing muscle or as satellite cells from quiescent muscle. In this study six rat pups yielded the myoblasts implanted into

27 injured hearts. In addition to their growth in culture, the myoblasts proliferated in vivo for several days after transplantation (Fig. 3 *E*). These properties have led us and several other groups to explore skeletal muscle grafting for cardiac repair. Koh et al. (7) demonstrated that the myogenic cell line C2C12 could be transplanted into the hearts of normal syngeneic mice, where the cells fused to form multinucleated myofibers. The same group also demonstrated that C2C12 cells stably transfected with a plasmid encoding active TGF-β could induce angiogenesis around the graft site (31). No coupling between the host cardiocytes and the grafted skeletal muscle was observed in either experiment.

Chiu et al. (8, 9) transplanted autologous satellite cells into cardiac freeze-thaw lesions in dogs. Comparable with our study, they also found that the grafts formed muscle cells within the healing lesion. In distinction to the current study, however, they hypothesized that their grafted skeletal muscle cells differentiated into cardiac muscle, via "milieu-dependent effects." The evidence for a cardiac phenotype was that some cells within the grafts had central rather than peripheral nuclei, and some cells contained refractile transverse structures under light microscopy interpreted to be intercalated discs. Although we observed some myofibers with persistent central nuclei in this study, as well as rare cells showing intermediate and gap junctions (Fig. 2, *C* and *D*), no intercalated discs were present by electron microscopy. More importantly, the grafted cells expressed skeletal muscle–specific proteins and failed to express the cardiac-specific isoform MHC-α up to 3 mo after transplantation. Thus, there clearly was no cardiac differentiation in this study.

Conversion of grafts from fast to slow twitch muscle. Although the skeletal muscle grafts expressed the fast fiber isoform of MHC at 1 and 2 wk, they expressed β-MHC, a marker for slow twitch fibers, at 7 wk and 3 mo. This indicates that the grafts were converting to slow twitch fibers. Conversion was apparently more rapid when the myoblasts were injected into wounds where healing had been allowed to progress for 1 wk, as opposed to immediately after injury. In the delayed transplantation model the grafts expressed β-MHC at 2 wk, while in the immediate transplantation model this protein was not detected until 7 wk. It is possible that the growth factors and cytokines present in the early wound delay myoblast differentiation and subsequent fiber type conversion.

Slow fibers exhibit several important differences from fast fibers, including a slower shortening velocity, use of oxidative phosphorylation for ATP production, a higher mitochondrial content, a higher myoglobin content, and a much greater resistance to fatigue (16, 32). An interesting parallel is that the latissimus dorsi muscle also undergoes fiber type switching when it is conditioned for dynamic cardiomyoplasty. Cardiomyoplasty is an experimental therapy for heart failure, where skeletal muscle is wrapped around the heart to serve as a ventricular assist device (33). Untrained latissimus dorsi is a mixed fiber type muscle which fatigues rapidly with repeated stimulation. When conditioned by repeated electrical stimulation for 6 wk before surgery, however, the latissimus dorsi converts entirely to slow twitch fibers and becomes fatigue resistant (6). Only the conditioned, slow twitch muscle is able to assist cardiac function. This parallel suggests the intriguing possibility that repeated electromechanical stimulation leads to activation of the slow fiber phenotype. Since we did not test whether the environment of the heart contributed to fiber type conversion, additional experiments will be required to determine the mechanism. The fact that the grafts differentiated into slow twitch fibers suggests that they may be suited to perform a cardiac type work load.

Will skeletal muscle transplantation augment cardiac function? This study definitively showed that myoblast grafting can generate new contractile tissue. The skeletal muscle grafts exhibited characteristic twitches when stimulated ex vivo (Fig. 4 *A*) and showed recruitment of contractile units with increasing voltage (Fig. 4 *B*). Furthermore, tetanus could be induced with rapid stimulation (Fig. 4 *A*, *second* and *third panels*), and the grafts could perform a cardiac-like duty cycle for 6 min (Fig. 4 *C*). Peak force during tetanus averaged 0.7±0.1 grams/mm^2. Since the wound strips contained < 50% of the myofiber content of normal muscle, due to inclusion of scar tissue, the force can be normalized to at least 1.4 grams/mm^2 muscle. Adult mammalian muscle can generate 15–35 grams/mm^2 force at tetanus, depending on fiber type (14, 34). Thus, the 2-wk grafts generated ~ 4–10% of the predicted force for mature skeletal muscle. Several factors may cause a lower than predicted force, including the relative immaturity of the 2-wk myofibers, stretching of the immature extracellular matrix, poor cell matrix attachments, or misalignment of some fibers relative to the axis of the wound strip.

Although preliminary, these results are encouraging and suggest that more detailed studies of contractile function are warranted in skeletal myoblast-engrafted hearts. A critical question is whether the skeletal muscle grafts contract in vivo. To provide coordinated mechanical assistance, the grafted cells ideally should form electrical and mechanical junctions with the host myocardium. In our grafts the skeletal muscle cells were insulated from the remaining myocardium by scar tissue, so there was no opportunity for myofiber–cardiocyte coupling to occur. Koh et al. (7) transplanted C2C12 myoblasts into normal mouse hearts and observed no cell junctions between grafted myofibers and host cardiocytes by electron microscopy. Although proliferating myoblasts have been reported to synthesize both gap junction proteins (35) and *N*-cadherin (36, 37), these proteins are typically absent from adult skeletal myofibers. By electron microscopy we observed evidence both for intermediate and gap junction formation between skeletal myofibers 2 wk after grafting (Fig. 2, *C* and *D*). This finding was infrequent, however, and it is unknown whether such junctions would persist in longer term grafts. If skeletal muscle will not couple spontaneously with cardiac muscle, it is possible that such junctions could be induced by stably transfecting skeletal muscle cells with genes for cardiac junctional proteins. Another possibility is that skeletal muscle grafts could be electrically paced in synchrony with the cardiac cycle. Pacing would require sufficient voltage to activate all of the fibers, and currently it is unknown whether this would have a deleterious effect on the surrounding myocardium.

In the uninjured heart there is a complex fiber geometry, where the outer fibers run in the long axis, the midwall fibers run in the short axis, and the inner fibers again run in the long axis. This geometry is established during embryogenesis and is thought to be important for mechanical efficiency. In this study, the grafted myofibers were predominantly aligned with the short (transverse) axis of the heart. Alignment was noted as early as day 3, when myotube formation was prominent (Fig. 1 *C*). This is the same orientation that wound fibroblasts and collagen fibers acquire during wound healing, and it seems

likely that all are aligned by local mechanical forces. It is not known whether alignment with the heart's short axis will influence the ability of these myofibers to restore mechanical function after injury.

There are two aspects of skeletal muscle which theoretically could make it superior to cardiac muscle for infarct repair. First, skeletal muscle is much more resistant to ischemia than cardiac muscle. Skeletal muscle can withstand many hours of severe ischemia without becoming irreversibly injured, whereas in myocardium irreversible injury begins within 20 min (38). A second difference is that skeletal myoblast grafts might establish satellite cells. Satellite cells are the resident stem cells in skeletal muscle and proliferate in response to injury. Once activated, satellite cells can fuse with damaged myofibers or establish new myofibers to replace those lost to necrosis. We observed cells within 2-wk grafts which were morphologically consistent with satellite cells by electron microscopy (Fig. 3, *E* and *F*). Thus, it is possible that infarcts repaired with skeletal myoblasts might become more resistant to a subsequent episode of ischemia or might be able to replace myofibers damaged by ischemia.

Acknowledgments

The authors are grateful for the adroit technical skills of Trudy Bartosek for performing all the immunocytochemistry, Cathy Gipaya for assistance with animal surgery, DeeAnn Gregory for assistance with myoblast culture, and Rene Collman for assistance with electron microscopy. The β-MHC antibody was a gift from Dr. Jeff Miller, Massachusetts General Hospital, Boston, MA. We thank Kelly Hudkins for her helpful advice for double immunostaining.

This study was supported in part by a Grant-in-Aid from the American Heart Association (C.E. Murry), and National Institutes of Health grants HL-03174 (S.M. Schwartz and S.D. Hauschka), HL-26405 (S.M. Schwartz), AR-18860 (S.D. Hauschka), and AR-41973 (R.W. Wiseman). Dr. Murry is the recipient of a Burroughs Wellcome Career Award in the Biomedical Sciences.

References

1. Reimer, K.A., and R.B. Jennings. 1979. The "wavefront phenomenon" of myocardial ischemic cell death. II. Transmural progression of necrosis within the framework of ischemic bed size (myocardium at risk) and collateral blood flow. *Lab. Invest.* 40:633–644.

2. Soonpaa, M.H., G.Y. Koh, M.G. Klug, and L.J. Field. 1994. Formation of nascent intercalated disks between grafted fetal cardiomyocytes and host myocardium. *Science (Wash. DC).* 264:98–101.

3. Koh, G.Y., M.H. Soonpaa, M.G. Klug, H.P. Pride, B.J. Cooper, D.P. Zipes, and L.J. Field. 1995. Stable fetal cardiomyocyte grafts in the hearts of dystrophic mice and dogs. *J. Clin. Invest.* 96:2034–2042.

4. Hauschka, S.D. 1974. Clonal analysis of vertebrate myogenesis. II. Environmental influences upon human muscle differentiation. *Dev. Biol.* 37:329–344.

5. Hauschka, S.D. 1982. Muscle cell culture: future goals for facilitating the investigation of human muscle disease. *In* Disorders of the Motor Unit. D.L. Schotland, editor. J. Wiley & Sons, New York. 925–936.

6. Mannion, J.D., T. Bitto, R.L. Hammond, N.A. Rubenstein, and L.W. Stephenson. 1986. Histochemical and fatigue characteristics of conditioned canine latissimus dorsi muscle. *Circ. Res.* 58:298–304.

7. Koh, G.Y., M.G. Klug, M.H. Soonpaa, and L.J. Field. 1993. Differentiation and long-term survival of C2C12 myoblast grafts in heart. *J. Clin. Invest.* 92:1548–1554.

8. Zibaitis, A., D. Greentree, F. Ma, D. Marelli, M. Duong, and R.C. Chiu. 1994. Myocardial regeneration with satellite cell implantation. *Transplant. Proc.* 26:3294.

9. Chiu, R.C., A. Zibaitis, and R.L. Kao. 1995. Cellular cardiomyoplasty: myocardial regeneration with satellite cell implantation. *Ann. Thorac. Surg.* 60: 12–18.

10. Clegg, C.H., and S.D. Hauschka. 1987. Heterokaryon analysis of muscle differentiation: regulation of the postmitotic state. *J. Cell Biol.* 105:937–947.

11. Vracko, R., and D. Thorning. 1991. Contractile cells in rat myocardial scar tissue. *Lab. Invest.* 65:214–227.

12. Vracko, R., D. Thorning, and R.G. Frederickson. 1990. Fate of nerve fibers in necrotic, healing and healed rat myocardium. *Lab. Invest.* 63:490–501.

13. Vracko, R., D. Thorning, R.G. Frederickson, and D. Cunningham. 1988. Myocyte reactions at the borders of injured and healing rat myocardium. *Lab. Invest.* 59:104–114.

14. Wiseman, R.W., T.W. Beck, and P.B. Chase. 1996. The effect of intracellular pH on force development depends on temperature in intact mouse skeletal muscle. *Am. J. Physiol.* 40:C878–C886.

15. Trupin, G.L., L. Hsu, and Y.-H. Hsieh. 1979. Satellite cell mimics in regenerating skeletal muscle. *In* Muscle Regeneration. A. Mauro, editor. Raven Press, New York. 101–114.

16. Kushmerick, M.J., T.S. Moerland, and R.W. Wiseman. 1992. Mammalian skeletal muscle fibers distinguished by contents of phosphocreatine, ATP, and Pi. *Proc. Natl. Acad. Sci. USA.* 89:7521–7525.

17. Quaini, F., E. Cigola, C. Lagrasta, G. Saccani, E. Quaini, C. Rossi, G. Olivetti, and P. Anversa. 1994. End-stage cardiac failure in humans is coupled with the induction of proliferating cell nuclear antigen and nuclear mitotic division in ventricular myocytes. *Circ. Res.* 75:1050–1063.

18. Rumyantsev, P.P. 1979. Some comparative aspects of myocardial regeneration. *In* Muscle Regeneration. A. Mauro, editor. Raven Press, New York. 335–355.

19. Reiss, K., J. Kajstura, J.M. Capasso, T.A. Marino, and P. Anversa. 1993. Impairment of myocyte contractility following coronary artery narrowing is associated with activation of the myocyte IGF1 autocrine system, enhanced expression of late growth related genes, DNA synthesis and myocyte nuclear mitotic division in rats. *Exp. Cell Res.* 207:348–360.

20. Tam, S.K.C., W. Gu, V. Mahdavi, and B. Nadal-Ginard. 1995. Cardiac myocyte terminal differentiation. *Ann. NY Acad. Sci.* 752:72–79.

21. Gu, W., J.W. Schneider, G. Condorelli, S. Kaushai, V. Mahdavi, and B. Nadal-Ginard. 1993. Interaction of myogenic factors and the retinoblastoma protein mediates muscle cell commitment and differentiation. *Cell.* 72:309–324.

22. Yoshizumi, M., W.S. Lee, C.M. Hsieh, J.C. Tsai, J. Li, M.A. Perrella, C. Patterson, W.A. Endege, R. Schlegel, and M.E. Lee. 1995. Disappearance of cyclin A correlates with permanent withdrawal of cardiomyocytes from the cell cycle in human and rat hearts. *J. Clin. Invest.* 95:2275–2280.

23. Kim, K.K., M.H. Soonpaa, A.I. Daud, G.Y. Koh, J.S. Kim, and L.J. Field. 1994. Tumor suppressor gene expression during normal and pathologic myocardial growth. *J. Biol. Chem.* 269:22607–22613.

24. Weintraub, H., R. Davis, S. Tapscott, M. Thayer, M. Krause, R. Benezra, T.K. Blackwell, D. Turner, R. Rupp, S. Hollenberg, et al. 1991. The MyoD gene family: nodal point during specification of the muscle cell lineage. *Science (Wash. DC).* 251:761–766.

25. Olson, E.N., and W.H. Klein. 1994. bHLH factors in muscle development: dead lines and commitments, what to leave in and what to leave out. *Genes Dev.* 8:1–8.

26. Murry, C.E., M.A. Kay, T. Bartosek, S.D. Hauschka, and S.M. Schwartz. 1996. Muscle differentiation during repair of myocardial necrosis in rats via gene transfer with MyoD. *J. Clin. Invest.* 98:2209–2217.

27. Prentice, H., R.A. Kloner, V. Sartorelli, S.D. Bellows, K. Alker, and L. Kedes. 1993. Transformation of cardiac fibroblasts into the skeletal muscle phenotype by injection of a MyoD-expressing retrovirus into ischemic heart. *Circulation.* 88(Suppl.):I475*a*. (Abstr.)

28. Murry, C.E., C. Fabre-Suver, S.D. Hauschka, and S.M. Schwartz. 1995. Skeletal and cardiac myoblast transplantation after myocardial necrosis: possible routes to muscle regeneration. *Circulation.* 92:I12*a*. (Abstr.)

29. Leor, R., M. Patterson, M.J. Quinones, L. Kedes, and R.A. Kloner. 1995. Successful transplantation of fetal cardiomyoblasts into the infarcted myocardium of rat: a potential method for repair of infarcted myocardium. *Circulation.* 92(Suppl.):I50*a*. (Abstr.)

30. Scorcin, M., F. Marotte, A. Sabri, O. Le Dref, M. Demirag, J.-L. Samuel, L. Rappaport, and P. Menasche. 1995. Can grafted cardiomyocytes colonize peri-infarction myocardial areas? *Circulation.* 92(Suppl.):I50*a*. (Abstr.)

31. Koh, G.Y., S.J. Kim, M.G. Klug, K. Park, M.H. Soonpaa, and L.J. Field. 1995. Targeted expression of transforming growth factor-beta 1 in intracardiac grafts promotes vascular endothelial cell DNA synthesis. *J. Clin. Invest.* 95:114–121.

32. Kelly, A.M., and N.A. Rubinstein. 1994. The diversity of muscle fiber types and its origin during development. *In* Myology. A.G. Engel and C. Franzini-Armstrong, editors. McGraw-Hill, New York. 119–133.

33. Niinami, H., A. Pochettino, and L.W. Stephenson. 1991. Use of skeletal muscle grafts for cardiac assist. *Trends Cardiovasc. Med.* 1:122–126.

34. Phillips, S.K., R.W. Wiseman, R.C. Woledge, and M.J. Kushmerick. 1993. The effects of metabolic fuel on force production and resting inorganic phosphate levels in mouse skeletal muscle. *J. Physiol. (Lond.).* 462:135–146.

35. Balogh, S., C.C.G. Naus, and P.A. Merrifield. 1993. Expression of gap junctions in cultured rat L6 cells during myogenesis. *Dev. Biol.* 155:351–360.

36. Cifuentes, D.C., M. Nicolet, D. Goudou, F. Reiger, and R.M. Mege. 1993. N-cadherin and N-CAM-mediated adhesion in development and regeneration of skeletal muscle. *Neuromuscul. Disord.* 3:361–365.

37. Mege, R.M., D. Goudou, D. Diaz, M. Nicolet, L. Garcia, G. Geraud,

and F. Rieger. 1992. N-cadherin and N-CAM in myoblast fusion: compared localisation and effect of blockade by peptides and antibodies. *J. Cell Sci.* 103: 897–906.

38. Jennings, R.B., and K.A. Reimer. 1981. Lethal myocardial ischemic injury. *Am. J. Pathol.* 102:241–255.

39. Bader, D., T. Masaki, and D.A. Fischman. 1982. Immunochemical analysis of myosin heavy chain during avian myogenesis in vivo and in vitro. *J. Cell Biol.* 95:763–770.

40. Havenith, M.G., R. Visser, J.M.C. Schrijvers-van Schendel, and F.T. Bosman. 1990. Muscle fiber typing in routinely processed skeletal muscle with monoclonal antibodies. *Histochemistry.* 93:497–499.

41. Rudnicki, M.A., G. Jackowski, L. Saggin, and M.W. McBurney. 1990. Actin and myosin expression during development of cardiac muscle from cultured embryonal carcinoma cells. *Dev. Biol.* 138:348–358.

42. Silberstein, L., S.G. Webster, M. Travis, and H.M. Blau. 1986. Developmental progression of myosin gene expression in cultured muscle cells. *Cell.* 46: 1075–1081.

43. Hughes, S.M., M. Cho, I. Karsch-Mizrachi, M. Travis, L. Silberstein, L.A. Leinwand, and H.M. Blau. 1993. Three slow myosin heavy chains sequentially expressed in developing mammalian skeletal muscle. *Dev. Biol.* 158:183–199.

44. Van Kleef, E.M., J.F.M. Smits, J.G.R. DeMey, J.P.M. Cleutjens, D.M. Lombardi, S.M. Schwartz, and M.J.A.P. Daemen. 1992. Alpha-1-adrenoreceptor blockade reduces the angiotensin II-induced vascular smooth muscle cell DNA synthesis in the rat thoracic aorta and carotid artery. *Circ. Res.* 70:1122–1127.